International Journal of Network Dynamics and Intelligence Scilight

Article

Privacy-Preserving Distributed Recursive Filtering for State-Saturated Systems with Quantization Effects

Youyin Hu, Chen Zhang, and Shuai Liu*

College of Science, University of Shanghai for Science and Technology, Shanghai 200093, China
* Correspondence: liushuai871030@163.com

Received: 16 February 2025
Accepted: 4 May 2025
Published: 30 June 2025

Abstract: This paper addresses the problem of distributed recursive filtering for state-saturated systems in a networked communication environment. An output mask function is employed to safeguard the privacy of interaction data during node exchange in sensor networks. Scaled uniform quantization is introduced to facilitate the digital communication and optimize the network resource usage. The primary objective of the study is to design a distributed recursive filter that ensures the filtering error covariance remains bounded over a finite horizon. Specifically, by using Riccati-like equations, an upper bound for the filtering error covariance is derived, which depends on the network topology, the output mask function, and the quantization level. The desired gain matrix is then solved recursively. Finally, the effectiveness of the proposed filtering algorithm is demonstrated through a three-tank simulation example.

Keywords: Distributed filtering; recursive filtering; privacy protection; uniform quantization; output mask

1. Introduction

With the rapid development of Internet of Things technology, sensor networks have received continuous attention from academia and industry due to their widespread applications in industrial monitoring, smart cities, environmental monitoring, and military surveillance [1, 2]. Sensor networks consist of a large number of spatially distributed intelligent nodes that can sense environmental information, process data, and communicate with neighboring nodes. In practical applications, sensor networks face challenges like limited node energy, constrained bandwidth, and harsh environmental conditions. As one of the fundamental problems in sensor networks, distributed state estimation aims to achieve accurate estimation of target states through local information interactions between nodes. However, in practical engineering, measurement data is often affected by various factors, such as measurement noise, sensor faults, communication delays, and data loss [3]. These uncertainty factors significantly degrade the system's estimation performance. Furthermore, limitations in communication resources between nodes and uncertainties in system models [4] all pose significant challenges to the design of distributed filters.

In recent years, various distributed filtering schemes have been proposed, which can effectively avoid computational bottlenecks and communication burden caused by centralized processing, while improving system scalability and fault tolerance. In practical applications, distributed filtering achieves global optimal estimation through local information interaction, greatly enhancing the overall system performance. For instance, consensus-based distributed Kalman filtering algorithms can achieve estimation consistency through iterative averaging between nodes [5]. The event-triggered-based distributed filtering [6] can effectively reduce network load while guaranteeing system performance. The robust distributed filtering methods considering model uncertainties [7] can enhance the system's adaptability to parameter perturbations. Moreover, H_∞ criterion-based distributed filtering can effectively handle bounded disturbances and modeling errors of the system, while improving the robustness of state estimation. Therefore, designing efficient and reliable distributed filtering algorithms is of great significance for improving the overall performance of sensor networks.

Since Rudolf Emil Kalman introduced state space into estimation theory in 1960 [8], Kalman filtering has become a powerful tool for solving state estimation problems in linear systems affected by Gaussian noises due to its favorable recursive attribute and reliable optimality assurance. Based on hidden Markov models and linear algebra, Kalman filtering can estimate states in real-time without storing all historical data, which significantly reduces computational resources and storage space requirements [9]. However, the conditions for the traditional Kalman filter are quite stringent, as it is only applicable to linear systems with Gaussian noises. Due to various uncertainties and nonlinear characteristics in practical systems, these conditions are often difficult to be satisfied, which limits the application scope of the Kalman filter [10]. To overcome this limitation, researchers have developed various improvement methods, among which the extended Kalman filter (EKF) is the most representative. The EKF extends the Kalman filter's capability to handle nonlinear problems by converting the original nonlinear system into an approximate linear system through the linearization technique [11]. It is particularly noteworthy that the EKF can effectively handle nonlinear problems related to process models, observation models, or both by performing linearization around current means and covariances [12]. Furthermore, the EKF is recognized as an efficient online (recursive) estimator of process variables, particularly suitable for scenarios where large numbers of parameters need to be identified using short time series. In recent years, the EKF has made significant progress in multiple fields, such as networked control systems, multi-agent systems [13], and wind turbine fault diagnosis [14].

Over the past few decades, with the rapid development of communication, computing, and control technologies, networked control systems (NCSs) have been widely applied in various fields such as industrial automation, intelligent manufacturing, and remote monitoring [15–18]. By connecting components such as controllers, sensors, and actuators through communication networks, NCSs enable remote transmission and processing of information, offering significant advantages including high flexibility, low cost, and easy maintenance. However, due to the complexity of network environments, NCSs inevitably face several challenges [19]. To efficiently utilize limited network resources, event-triggered mechanisms have been widely adopted in NCSs [20, 21], which can dynamically determine data transmission times based on changes in system states, thereby reducing unnecessary network communication. Furthermore, limited network bandwidth results in network congestion, communication delays [22, 23], and signal distortion, which inevitably affect system performance.

To effectively address the challenge of bandwidth constraints, the quantization technique has been introduced into NCSs as a data compression method [24–26]. In the quantization process, the sender first maps continuous raw data to a finite set of discrete values, which are transmitted through communication networks and then reconstructed at the receiver end as approximations of the original data. Current main quantization strategies include uniform quantization and logarithmic quantization, among which uniform quantization has been widely adopted due to its simple implementation and high computational efficiency. However, the design of quantization systems faces multiple challenges. First, the selection of quantization parameters (such as quantization intervals and levels) directly affects the trade-off between communication efficiency and signal reconstruction accuracy. Second, due to the nonlinear characteristics of the quantization process [27], quantization errors are inevitablely accumulated over time that leads to system performance degradation. Furthermore, in practical applications, systems may face uncertainty factors such as measurement noises and external disturbances, which further increases the complexity of quantizer design.

With the widespread application of sensor networks in distributed computing, intelligent transportation systems, and smart grids, information exchange between nodes inevitably brings risks of privacy leakage. Currently, the mainstream privacy protection strategies mainly include two methods: differential privacy and homomorphic encryption. Differential privacy protects sensitive information by adding well-designed noises to transmission signals, which is simple to implement and has a low computational burden. However, existing research has shown that consensus algorithms based on differential privacy cannot achieve exact convergence [28, 29], which is unacceptable in certain high-precision application scenarios (such as microgrid voltage control) [30]. Homomorphic encryption ensures data security by converting information into ciphertext. Although Homomorphic encryption can guarantee absolute information security, it requires the transmission of additional public key information, resulting in significantly increased communication overhead. Particularly in large-scale distributed systems, as the number of nodes increases, the communication burden rises dramatically [31]. In recent years, output mask has gained attention as a novel privacy protection method [32]. This approach protects initial states by superimposing dynamically vanishing mask functions on the original state information [33, 34], which can achieve exact convergence without requiring additional communication bandwidth.

In this paper, we aim to develop a distributed recursive filter for state-saturated systems in a networked communication environment. The main contributions of this paper can be summarized as follows. 1) To safeguard the privacy of interaction data, an output mask function is, for the first time, introduced to the state-saturated systems over sensor networks. 2) A novel distributed recursive filter is designed under which the filtering error covariance remains bounded over a finite horizon by using Riccati-like equations. 3) An upper bound for the filtering error covariance is derived, which depends on the network topology, the output mask function, and the quantization level.

Notations: $\mathbb{R}^+$, $\mathbb{R}^m$ are the set of non-negative real numbers and the m-dimensional Euclidean space, respectively. $\|\cdot\|$ represents the Euclidean norm. The superscript M^{T} stands for the transpose of the matrix M. I represents the identity matrix with appropriate dimensions. $\mathbb{E}\{x\}$ stand for the mean of any stochastic variable x.

2. Problem Formulation

2.1. Graph theory

In this paper, the system output measurement is accomplished through a sensor network consisting of N sensor nodes. The topology of this sensor network can be described by a directed graph $\mathcal{G} = (\mathcal{V}, \mathcal{E}, \mathcal{A})$ of order N. Here, $\mathcal{V} = \{1, 2, \cdots, N\}$ represents the set of sensor nodes, $\mathcal{E} \subseteq \mathcal{V} \times \mathcal{V}$ denotes the set of directed edges, and $\mathcal{A} = [a_{ij}]_{N\times N}$ is the weighted adjacency matrix of graph $\mathcal{G}$. The elements of adjacency matrix $\mathcal{A}$ are nonnegative, and there exists a directed edge $(i, j) \in \mathcal{E}$ if and only if $a_{ij} > 0$, which indicates that the ith sensor node can receive information from the jth sensor node, in which case node j is called a neighbor of node i. For notational convenience, the set of neighbors of node i (including node i itself) is denoted by $\mathcal{N}_i = \{j \in \mathcal{V} | (i, j) \in \mathcal{E}\}$. Based on this topology, each sensor node can collect system data and exchange information with its neighboring nodes. In particular, when there exists a connection between any two nodes $i, j \in \mathcal{V}$ in graph $\mathcal{G}$, the communication graph is called completely connected.

2.2. System model

We consider the following discrete-time stochastic nonlinear state-saturated systems:

$$\begin{cases} x_{k+1} = \sigma(\mathbf{f}(x_k)) + w_k \\ y_{i,k} = \mathbf{g}_i(x_k) + v_{i,k} \end{cases} \tag{1}$$

where $x_k \in \mathbb{R}^n$ and $y_{i,k} \in \mathbb{R}^m$ are, respectively, the system state to be estimated and the measurement output measured by the sensor i. $w_k \in \mathbb{R}^n$ and $v_{i,k} \in \mathbb{R}^m$ are two zero-mean white noise sequences with the covariances $\mathbf{Q}_k$ and $\mathbf{R}_{i,k}$, respectively. It is assumed that all noises are uncorrelated and bounded by $\|w_k\| \leqslant \bar{w}$ and $\|v_{i,k}\| \leqslant \bar{v}$ with $\bar{w}$ and $\bar{v}$ being the known positive constants, which are also uncorrelated with the initial state. The nonlinear functions $\mathbf{f}(\cdot) : \mathbb{R}^n \to \mathbb{R}^n$ and $\mathbf{g}_i(\cdot) : \mathbb{R}^n \to \mathbb{R}^m$ are known and continuously differentiable. The saturation function $\sigma(\cdot) : \mathbb{R}^n \mapsto \mathbb{R}^n$ is defined as

$$\sigma(z) = [\sigma_1(z_1)\ \sigma_2(z_2)\ \cdots\ \sigma_n(z_n)]^T \tag{2}$$

where

$$\sigma_i(z_i) = \mathrm{sign}(z_i) \min\{z_{i,\max}, |z_i|\} \tag{3}$$

and $z_{i,\max}$ is the ith element of the vector $z_{\max}$ (i.e., the saturation level).

2.3. Output Mask Privacy-Preserving Method

The basic principle of the output mask approach is to avoid leaking the initial value of the exchanged information and keep the initial attractor convergence by inserting a dynamic vanished mask function [33].

As described in [33], define the map function $\mathbf{h}_i(\cdot,\cdot,\cdot) : \mathbb{R}^+ \times \mathbb{R}^m \times \mathbb{R}^m \mapsto \mathbb{R}^m$, $i = 1, 2, \cdots, m$. Accordingly, the output mask function is defined as

$$\bar{y}_{i,k} = \mathbf{h}_i(k, y_{i,k}, \phi_i) = (1 + \psi_i \mathrm{e}^{-\nu_i k})(y_{i,k} + \theta_i \mathrm{e}^{-\epsilon_i k}) \tag{4}$$

where $\phi_i \triangleq \{\psi_i, \nu_i, \theta_i, \epsilon_i\}$, ψ_i, ν_i and ϵ_i are given positive scalars, $\theta_i \in \mathbb{R}^m$ is a non-zero vector. It is worth noting that the internal parameters of the output mask $\mathbf{h}_i(\cdot,\cdot,\cdot)$ are also private to the other nodes, and parameters ψ_i, ν_i, θ_i and ϵ_i are independently decided by the node i, which implies that node j in the network cannot deduce the precise state value of node i based on the received information.

Before the signals enter into the digital network, the uniform quantization technique is adopted to encode the analogy signals to the digital signals. The following uniform quantizer is used:

$$\mathbf{q}(\chi) = \begin{cases} M, & \chi \geqslant M \\ -M, & \chi < -M \\ -M + \dfrac{(2t-1)M}{\rho}, & -M + \dfrac{2(t-1)M}{\rho} \leqslant \chi < -M + \dfrac{2tM}{\rho}, \ \ t = 1, 2, \cdots, \rho \end{cases} \tag{5}$$

where χ is the signal to be quantized and M is the saturated bound. The interval $[-M, M]$ is partitioned into ρ

regions.

For the measurement component $\bar{y}_{i,k}^{(s)}$ $(s = 1,2,\cdots,m)$, define $\mathbf{q}_s\left(\bar{y}_{i,k}^{(s)}\right) \triangleq \varrho_{i,k}^{(s)}\mathbf{q}\left(\frac{\bar{y}_{i,k}^{(s)}}{\varrho_{i,k}^{(s)}}\right)$ where $\varrho_{i,k}^{(s)} > 0$ is an adjustable parameter. In order to address the issue of quantization saturation of $\mathbf{q}_s(\cdot)$, the parameter $\varrho_{i,k}^{(s)}$ is selected to ensure that the value $\frac{\bar{y}_{i,k}^{(s)}}{\varrho_{i,k}^{(s)}}$ enters into the interval $[-M,M]$ when $\left|\bar{y}_{i,k}^{(s)}\right| > M$. Therefore, it is easy to derive that the quantization error $\xi_{i,k}^{(s)} \triangleq \bar{y}_{i,k}^{(s)} - \mathbf{q}_s\left(\bar{y}_{i,k}^{(s)}\right)$ satisfying

$$\left|\xi_{i,k}^{(s)}\right| \leqslant \frac{\varrho_{i,k}^{(s)}M}{\rho}. \tag{6}$$

Define

$$\begin{aligned}\bar{\mathbf{q}}(\bar{y}_{i,k}) &\triangleq \mathrm{col}\left\{\mathbf{q}_1(\bar{y}_{i,k}^{(1)}), \mathbf{q}_2(\bar{y}_{i,k}^{(2)}), \cdots, \mathbf{q}_m(\bar{y}_{i,k}^{(m)})\right\}\\ \xi_{i,k} &\triangleq \mathrm{col}\left\{\xi_{i,k}^{(1)}, \xi_{i,k}^{(2)}, \cdots, \xi_{i,k}^{(m)}\right\}\\ \varrho_{i,k} &\triangleq \mathrm{col}\left\{\varrho_{i,k}^{(1)}, \varrho_{i,k}^{(2)}, \cdots, \varrho_{i,k}^{(m)}\right\}.\end{aligned}$$

Based on the obtained quantization measurement, the following robust Kalman-type filter is designed:

$$\hat{x}_{i,k+1}^- = \sigma(\mathbf{f}(\hat{x}_{i,k|k}^+)) \tag{7}$$

$$\hat{x}_{i,k+1}^+ = \hat{x}_{i,k+1}^- + \sum_{j=1}^{N}\mathbf{K}_{ij,k+1}a_{ij}\left(\bar{\mathbf{q}}(\bar{y}_{j,k+1}) - \mathbf{h}_j(k+1, \hat{y}_{i,k+1}^-, \phi_i)\right) \tag{8}$$

where $\hat{x}_{i,k+1}^- \in \mathbb{R}^n$ is the one-step prediction of x_{k+1} for node i at time k, $\hat{x}_{i,k+1}^+ \in \mathbb{R}^n$ is the estimation of x_{k+1} at time $k+1$, $\hat{y}_{i,k+1}^-$ is the prediction of y_{k+1} defined by $\hat{y}_{i,k+1}^- \triangleq \mathbf{g}_i(\hat{x}_{i,k+1}^-)$, and $\mathbf{K}_{ij,k+1}$ is the filter gain matrix to be determined.

The main purpose of this paper can be summarized as follows. For the state-saturated stochastic nonlinear systems subject to the privacy protection and the signal quantization, there exists a sequence of positive-definite matrices $\mathbf{\Sigma}_{i,k}^+$ such that the filtering error satisfies the following inequality constraints:

$$\mathbb{E}\{(x_k - \hat{x}_{i,k}^+)(x_k - \hat{x}_{i,k}^+)^T\} \leqslant \mathbf{\Sigma}_{i,k}^+. \tag{9}$$

Moreover, the filter parameter $\mathbf{K}_{ij,k}$ can be derived by minimizing the upper bound $\mathbf{\Sigma}_{i,k}^+$.

3. Main results

Lemma 1 *For $\forall x_1,\ x_2 \in \mathbb{R}$, there exists a real number $\varepsilon_i \in [0,\ 1]$ such that*

$$\sigma_i(x_1) - \sigma_i(x_2) = \varepsilon_i(x_1 - x_2) \tag{10}$$

where $\sigma_i(\cdot)$ $(i = 1,2,\cdots,n)$ is the saturation function defined in (2).

Lemma 2 *[33] Let the matrices A, B, C and Λ be given with appropriate dimensions and satisfy $\Lambda\Lambda^T \leqslant I$. For any positive definite matrix Z and any positive constant α, if the condition $\alpha^{-1}I - CZC^T > 0$ is satisfied, the following inequality holds*

$$(A + B\Lambda C)Z(A + B\Lambda C)^T \leqslant A(Z^{-1} - \alpha C^TC)^{-1}A^T + \alpha^{-1}BB^T. \tag{11}$$

Define the estimation error $\tilde{x}_{i,k}^+ \triangleq x_k - \hat{x}_{i,k}^+$ and the one-step prediction error $\tilde{x}_{i,k+1}^- \triangleq x_{k+1} - \hat{x}_{i,k+1}^-$. Based on Lemma 1, it follows from (1) and (7) that the one-step prediction error can be computed as

$$\begin{aligned}\tilde{x}_{i,k+1}^- &= \sigma(\mathbf{f}(x_k)) + w_k - \sigma(\mathbf{f}(\hat{x}_{i,k}^+))\\ &= \Upsilon_{i,k}\left(\mathbf{f}(x_k) - \mathbf{f}(\hat{x}_{i,k}^+)\right) + w_k\end{aligned} \tag{12}$$

and the estimation error can be derived as

$$
\begin{aligned}
\tilde{x}^{+}_{i,k+1} =& \tilde{x}^{-}_{i,k+1} - \sum_{j=1}^{N} \mathbf{K}_{ij,k+1} a_{ij} \left(\bar{\mathbf{q}}(\bar{y}_{j,k+1}) - \mathbf{h}_j(k+1, \hat{y}^{-}_{i,k+1}, \phi_i) \right) \\
=& \tilde{x}^{-}_{i,k+1} - \sum_{j=1}^{N} \mathbf{K}_{ij,k+1} a_{ij} \left(\bar{\mathbf{q}}(\bar{y}_{j,k+1}) - \bar{y}_{j,k+1} + \bar{y}_{j,k+1} - \mathbf{h}_j(k+1, \hat{y}^{-}_{i,k+1}, \phi_i) \right) \\
=& \tilde{x}^{-}_{i,k+1} - \sum_{j=1}^{N} \mathbf{K}_{ij,k+1} a_{ij} \left(\left(1 + \psi_j \mathrm{e}^{-\nu_j(k+1)}\right) \left(\mathbf{g}_j(x_{k+1}) + v_{j,k+1} + \theta_j \mathrm{e}^{-\epsilon_j(k+1)} \right) \right. \\
& \left. - \left(1 + \psi_j \mathrm{e}^{-\nu_j(k+1)}\right) \left(\mathbf{g}_j(\hat{x}^{-}_{j,k+1}) + \theta_j \mathrm{e}^{-\epsilon_j(k+1)} \right) - \xi_{j,k+1} \right) \\
=& \tilde{x}^{-}_{i,k+1} - \sum_{j=1}^{N} \mathbf{K}_{ij,k+1} a_{ij} \left(\left(1 + \psi_j \mathrm{e}^{-\nu_j(k+1)}\right) \left(\mathbf{g}_j(x_{k+1}) - \mathbf{g}_j(\hat{x}^{-}_{j,k+1}) + v_{j,k+1} \right) - \xi_{j,k+1} \right)
\end{aligned}
\tag{13}
$$

where

$$
\Upsilon_{i,k} \triangleq \operatorname{diag}\left\{ \varepsilon^{(1)}_{i,k}, \varepsilon^{(2)}_{i,k}, \cdots, \varepsilon^{(n)}_{i,k} \right\}.
$$

The Taylor expansion of the function $f(\cdot)$ at the point $\hat{x}^{+}_{i,k}$ yields

$$
\mathbf{f}(x_k) = f(\hat{x}_{i,k|k}) + \mathbf{A}_{i,k} \tilde{x}^{+}_{i,k} + \mathbf{G}_{i,k} \Gamma_k \mathbf{H}_{i,k} \tilde{x}^{+}_{i,k} \tag{14}
$$

where $\mathbf{A}_{i,k} \triangleq \left.\dfrac{\partial \mathbf{f}}{\partial x}\right|_{x=\hat{x}^{+}_{i,k}}$ denotes the Jacobian matrix. $\mathbf{G}_{i,k} \Gamma_k \mathbf{H}_{i,k} \tilde{x}^{+}_{i,k}$ is used to represent the linearization error. $\mathbf{G}_{i,k}$ and $\mathbf{H}_{i,k}$ are known matrices dependent on $\hat{x}^{+}_{i,k} \Gamma_k$ is an unknown matrix satisfying the following norm-bounded uncertainty:

$$
\Gamma_k \Gamma_k^T \leqslant I. \tag{15}
$$

Along the same line, the nonlinear function $g_i(\cdot)$ is expanded at the point $\hat{x}^{-}_{i,k+1}$, thus leading to

$$
\mathbf{g}_i(x_{k+1}) = \mathbf{g}_i(\hat{x}^{-}_{i,k+1}) + \mathbf{C}_{i,k+1} \tilde{x}^{-}_{i,k+1} + \bar{\mathbf{G}}_{i,k+1} \bar{\Gamma}_{i,k+1} \bar{\mathbf{H}}_{i,k+1} \tilde{x}^{-}_{i,k+1} \tag{16}
$$

where $\mathbf{C}_{i,k+1} \triangleq \left.\dfrac{\partial \mathbf{g}_i}{\partial x}\right|_{x=\hat{x}^{-}_{i,k+1}}$ denotes the Jacobian matrix. $\bar{\mathbf{G}}_{k+1} \bar{\Gamma}_{k+1} \bar{\mathbf{H}}_{k+1} \tilde{x}^{-}_{i,k+1}$ is used to represent the linearization error. $\bar{\mathbf{G}}_{k+1}$ and $\bar{\mathbf{H}}_{k+1}$ are known matrices dependent on $\hat{x}^{-}_{i,k+1}$. $\bar{\Gamma}_{i,k+1}$ is an unknown matrix satisfying the following norm-bounded uncertainty:

$$
\bar{\Gamma}_{i,k+1} \bar{\Gamma}^{T}_{i,k+1} \leqslant I. \tag{17}
$$

Therefore, the one-step prediction error and the estimation error can, respectively, be rewritten as

$$
\tilde{x}^{-}_{i,k+1} = \Upsilon_{i,k} (\mathbf{A}_{i,k} + \mathbf{G}_k \Gamma_k \mathbf{H}_k) \tilde{x}^{+}_{i,k} + w_k \tag{18}
$$

and the estimation error can be derived as

$$
\tilde{x}^{+}_{i,k+1} = \tilde{x}^{-}_{i,k+1} - \sum_{j=1}^{N} \mathbf{K}_{ij,k+1} a_{ij} \left(\left(1 + \psi_j \mathrm{e}^{-\nu_j(k+1)}\right) \left((\mathbf{C}_{j,k+1} + \bar{\mathbf{G}}_{j,k+1} \bar{\Gamma}_{j,k+1} \bar{\mathbf{H}}_{j,k+1}) \tilde{x}^{-}_{j,k+1} + v_{j,k+1} \right) - \xi_{j,k+1} \right). \tag{19}
$$

Define the following notations:

$$
\begin{aligned}
\tilde{x}^{+}_{k+1} &\triangleq \operatorname{col}\{\tilde{x}^{+}_{1,k+1}, \tilde{x}^{+}_{2,k+1}, \cdots, \tilde{x}^{+}_{N,k+1}\} \\
\tilde{x}^{-}_{k+1|k} &\triangleq \operatorname{col}\{\tilde{x}^{-}_{1,k+1}, \tilde{x}^{-}_{2,k+1}, \cdots, \tilde{x}^{-}_{N,k+1}\} \\
\mathbf{\Psi}_{k+1} &\triangleq \operatorname{diag}\{1 + \psi_1 \mathrm{e}^{-\nu_1(k+1)}, \cdots, 1 + \psi_N \mathrm{e}^{-\nu_N(k+1)}\} \otimes I_m \\
\vec{\mathbf{A}}_k &\triangleq \operatorname{diag}\{\mathbf{A}_{1,k}, \mathbf{A}_{2,k}, \cdots, \mathbf{A}_{N,k}\} \\
\vec{\mathbf{G}}_k &\triangleq \operatorname{diag}\{\mathbf{G}_{1,k}, \mathbf{G}_{2,k}, \cdots, \mathbf{G}_{N,k}\} \\
\vec{\mathbf{H}}_k &\triangleq \operatorname{diag}\{\mathbf{H}_{1,k}, \mathbf{H}_{2,k}, \cdots, \mathbf{H}_{N,k}\} \\
\Upsilon_k &\triangleq \operatorname{diag}\{\Upsilon_{1,k}, \Upsilon_{2,k}, \cdots, \Upsilon_{N,k}\} \\
\bar{w}_k &\triangleq \operatorname{col}\{w_k, w_k, \cdots, w_k\} \\
\mathcal{A}_i &\triangleq \operatorname{diag}\{a_{i1}, a_{i2}, \cdots, a_{iN}\}
\end{aligned}
$$

$$
\begin{aligned}
\mathbf{K}_{k+1} &\triangleq [\mathbf{K}_{ij,k+1}]_{N\times N},\ \vec{\Gamma}_k \triangleq I_N \otimes \Gamma_k \\
\mathbf{C}_{k+1} &\triangleq \mathrm{diag}\{\mathbf{C}_{1,k+1}, \mathbf{C}_{2,k+1}, \cdots, \mathbf{C}_{N,k+1}\} \\
\bar{\mathbf{G}}_{k+1} &\triangleq \mathrm{diag}\{\bar{\mathbf{G}}_{1,k+1}, \bar{\mathbf{G}}_{2,k+1}, \cdots, \bar{\mathbf{G}}_{N,k+1}\} \\
\bar{\Gamma}_{k+1} &\triangleq \mathrm{diag}\{\bar{\Gamma}_{1,k+1}, \bar{\Gamma}_{2,k+1}, \cdots, \bar{\Gamma}_{N,k+1}\} \\
\bar{\mathbf{H}}_{k+1} &\triangleq \mathrm{diag}\{\bar{\mathbf{H}}_{1,k+1}, \bar{\mathbf{H}}_{2,k+1}, \cdots, \bar{\mathbf{H}}_{N,k+1}\} \\
v_{k+1} &\triangleq \mathrm{col}\{v_{1,k+1}, v_{2,k+1}, \cdots, v_{N,k+1}\} \\
\xi_{k+1} &\triangleq \mathrm{col}\{\xi_{1,k+1}, \xi_{2,k+1}, \cdots, \xi_{N,k+1}\} \\
\mathbf{E}_i &\triangleq \mathrm{diag}\{\underbrace{0, \cdots, 0}_{i-1}, I, \underbrace{0, \cdots, 0}_{N-i}\}.
\end{aligned}
$$

The compact form of (18) and (19) can be further written as

$$
\tilde{x}^-_{k+1} = \Upsilon_k(\vec{\mathbf{A}}_k + \vec{\mathbf{G}}_k\vec{\Gamma}_k\vec{\mathbf{H}}_k)\tilde{x}^+_k + \bar{w}_k \tag{20}
$$

and

$$
\begin{aligned}
\tilde{x}^+_{k+1} =&(I - \sum_{i=1}^{N}\mathbf{E}_i\mathbf{K}_{k+1}\mathcal{A}_i\mathbf{\Psi}_{k+1}\mathbf{C}_{k+1} - \sum_{i=1}^{N}\mathbf{E}_i\mathbf{K}_{k+1}\mathcal{A}_i\mathbf{\Psi}_{k+1}\bar{\mathbf{G}}_{k+1}\bar{\Gamma}_{k+1}\bar{\mathbf{H}}_{k+1})\tilde{x}^-_{k+1} \\
&- \sum_{i=1}^{N}\mathbf{E}_i\mathbf{K}_{k+1}\mathcal{A}_i\mathbf{\Psi}_{k+1}v_{k+1} + \sum_{i=1}^{N}\mathbf{E}_i\mathbf{K}_{k+1}\mathcal{A}_i\xi_{k+1}.
\end{aligned} \tag{21}
$$

Define the one-step prediction error covariance $\mathbf{P}^-_k \triangleq \mathbb{E}\{\tilde{x}^-_k(\tilde{x}^-_k)^T\}$ and the estimation error covariance $\mathbf{P}^+_k \triangleq \mathbb{E}\{\tilde{x}^+_k(\tilde{x}^+_k)^T\}$. Next, we shall give some results to calculate the recursive algorithm of the one-step error covariance and the estimation error covariance.

Theorem 1 *For given scalars α_1, α_2, κ, considering the error dynamics* (20)–(21)*, the upper bound of the one-step prediction error covariance $\mathbf{P}^-_{k+1}$ and the estimation error covariance $\mathbf{P}^+_{k+1}$ obey the following recursions:*

$$
\mathbf{\Sigma}^-_{k+1} = \Upsilon_k[\vec{\mathbf{A}}_k((\mathbf{\Sigma}^+_k)^{-1} - \alpha_1\vec{\mathbf{H}}^T_k\vec{\mathbf{H}}_k)^{-1}\vec{\mathbf{A}}_k + \alpha_1^{-1}\vec{\mathbf{G}}_k\vec{\mathbf{G}}^T_k]\Upsilon^T_k + \bar{\mathbf{Q}}_k \tag{22}
$$

and

$$
\mathbf{\Sigma}^+_{k+1} = \varpi_1(I + \mathcal{K}_{k+1}\mathbf{\Psi}_k\mathbf{C}_{k+1})((\mathbf{\Sigma}^-_{k+1})^{-1} - \alpha_2\bar{\mathbf{H}}^T_{k+1}\bar{\mathbf{H}}_{k+1})^{-1}(I + \mathcal{K}_{k+1}\mathbf{\Psi}_k\mathbf{C}_{k+1})^T + \mathcal{K}_{k+1}\mathbf{U}_{k+1}\mathcal{K}^T_{k+1} \tag{23}
$$

with the following constraints

$$
\alpha_1^{-1}I - \vec{\mathbf{H}}_k\mathbf{\Sigma}^+_k\vec{\mathbf{H}}^T_k > 0 \tag{24}
$$

$$
\alpha_2^{-1}I - \bar{\mathbf{H}}_{k+1}\mathbf{\Sigma}^-_{k+1}\bar{\mathbf{H}}^T_{k+1} > 0 \tag{25}
$$

where

$$
\begin{aligned}
\mathbf{U}_{k+1} &\triangleq \varpi_1\alpha_2^{-1}\mathbf{\Psi}_{k+1}\bar{\mathbf{G}}_{k+1}\bar{\mathbf{G}}^T_{k+1}\mathbf{\Psi}^T_{k+1} + \mathbf{\Psi}_{k+1}\mathcal{R}_{k+1}\mathbf{\Psi}^T_{k+1} + \varpi_2\vec{\varrho}_k I_{Nm} \\
\mathcal{R}_{k+1} &\triangleq \mathrm{diag}\{\mathbf{R}_{1,k+1}, \mathbf{R}_{2,k+1}, \cdots, \mathbf{R}_{N,k+1}\} \\
\varpi_1 &\triangleq 1 + \kappa, \varpi_2 \triangleq 1 + \kappa^{-1},\ \bar{\mathbf{Q}}_k \triangleq I_N \otimes \mathbf{Q}_k \\
\bar{\varrho}_k &\triangleq \mathrm{col}\{\varrho_{1,k}, \varrho_{2,k}, \cdots, \varrho_{m,k}\} \otimes \frac{M}{\rho},\ \vec{\varrho}_k \triangleq \bar{\varrho}^T_k\bar{\varrho}_k.
\end{aligned}
$$

Proof of Theorem 1. First, according to the error dynamics (20), it is easy to obtain that

$$
\begin{aligned}
\mathbf{P}^-_{k+1} &\triangleq \mathbb{E}\{\tilde{x}^-_{k+1}(\tilde{x}^-_{k+1})^T\} \\
&= \Upsilon_k(\vec{\mathbf{A}}_k + \vec{\mathbf{G}}_k\vec{\Gamma}_k\vec{\mathbf{H}}_k)\mathbf{P}^+_k(\vec{\mathbf{A}}_k + \vec{\mathbf{G}}_k\vec{\Gamma}_k\vec{\mathbf{H}}_k)^T\Upsilon^T_k + \bar{\mathbf{Q}}_k.
\end{aligned} \tag{26}
$$

Based on Lemma 2, we can derive the following inequality:

$$
\mathbf{P}^-_{k+1} \leqslant \Upsilon_k[\vec{\mathbf{A}}_k((\mathbf{P}^+_k)^{-1} - \alpha_1\vec{\mathbf{H}}^T_k\vec{\mathbf{H}}_k)^{-1}\vec{\mathbf{A}}_k + \alpha_1^{-1}\vec{\mathbf{G}}_k\vec{\mathbf{G}}^T_k]\Upsilon^T_k + \bar{\mathbf{Q}}_k. \tag{27}
$$

By defining $\mathcal{K}_{k+1} = -\sum_{i=1}^{N}\mathbf{E}_i\mathbf{K}_{k+1}\mathcal{A}_i$, we can obtain from (21) that

$$
\begin{aligned}
\tilde{x}^+_{k+1} =&(I + \mathcal{K}_{k+1}\mathbf{\Psi}_{k+1}\mathbf{C}_{k+1} + \mathcal{K}_{k+1}\mathbf{\Psi}_{k+1}\bar{\mathbf{G}}_{k+1}\bar{\Gamma}_{k+1}\bar{\mathbf{H}}_{k+1})\tilde{x}^-_{k+1} \\
&+ \mathcal{K}_{k+1}\mathbf{\Psi}_{k+1}v_{k+1} - \mathcal{K}_{k+1}\xi_{k+1}.
\end{aligned} \tag{28}
$$

Further, we have

$$\begin{aligned}\mathbf{P}^{+}_{k+1} \triangleq&\mathbb{E}\{\tilde{x}^{+}_{k+1}(\tilde{x}^{+}_{k+1})^{T}\}\\ =&\mathbb{E}\left\{((I+\mathcal{K}_{k+1}\mathbf{\Psi}_{k+1}\mathbf{C}_{k+1}+\mathcal{K}_{k+1}\mathbf{\Psi}_{k+1}\bar{\mathbf{G}}_{k+1}\bar{\Gamma}_{k+1}\bar{\mathbf{H}}_{k+1})\tilde{x}^{-}_{k+1}\right.\\ &+\mathcal{K}_{k+1}\mathbf{\Psi}_{k+1}v_{k+1}-\mathcal{K}_{k+1}\xi_{k+1})\\ &\times((I+\mathcal{K}_{k+1}\mathbf{\Psi}_{k+1}\mathbf{C}_{k+1}+\mathcal{K}_{k+1}\mathbf{\Psi}_{k+1}\bar{\mathbf{G}}_{k+1}\bar{\Gamma}_{k+1}\bar{\mathbf{H}}_{k+1})\tilde{x}^{-}_{k+1}\\ &\left.+\mathcal{K}_{k+1}\mathbf{\Psi}_{k+1}v_{k+1}-\mathcal{K}_{k+1}\xi_{k+1})\right\}.\end{aligned}\tag{29}$$

Based on the fundamental inequality

$$xy^{T}+yx^{T}\leqslant\epsilon xx^{T}+\epsilon^{-1}yy^{T}\tag{30}$$

for any vectors x, y and any positive scalar ϵ, we have

$$\begin{aligned}\mathbf{P}^{+}_{k+1}\leqslant&\varpi_{1}(I+\mathcal{K}_{k+1}\mathbf{\Psi}_{k+1}\mathbf{C}_{k+1}+\mathcal{K}_{k+1}\mathbf{\Psi}_{k+1}\bar{\mathbf{G}}_{k+1}\bar{\Gamma}_{k+1}\bar{\mathbf{H}}_{k+1})\mathbf{P}^{-}_{k+1}\\ &\times(I+\mathcal{K}_{k+1}\mathbf{\Psi}_{k+1}\mathbf{C}_{k+1}+\mathcal{K}_{k+1}\mathbf{\Psi}_{k+1}\bar{\mathbf{G}}_{k+1}\bar{\Gamma}_{k+1}\bar{\mathbf{H}}_{k+1})^{T}\\ &+\varpi_{2}\mathcal{K}_{k+1}\xi_{k+1}\xi^{T}_{k+1}\mathcal{K}^{T}_{k+1}+\mathcal{K}_{k+1}\mathbf{\Psi}_{k+1}\mathcal{R}_{k+1}\mathbf{\Psi}^{T}_{k+1}\mathcal{K}^{T}_{k+1}.\end{aligned}\tag{31}$$

Then, according to Lemma 2, we have

$$\begin{aligned}\mathbf{P}^{+}_{k+1}\leqslant&\varpi_{1}(I+\mathcal{K}_{k+1}\mathbf{\Psi}_{k+1}\mathbf{C}_{k+1}+\mathcal{K}_{k+1}\mathbf{\Psi}_{k+1}\bar{\mathbf{G}}_{k+1}\bar{\Gamma}_{k+1}\bar{\mathbf{H}}_{k+1})\mathbf{P}^{-}_{k+1}\\ &\times(I+\mathcal{K}_{k+1}\mathbf{\Psi}_{k+1}\mathbf{C}_{k+1}+\mathcal{K}_{k+1}\mathbf{\Psi}_{k+1}\bar{\mathbf{G}}_{k+1}\bar{\Gamma}_{k+1}\bar{\mathbf{H}}_{k+1})^{T}\\ &+\varpi_{2}\mathcal{K}_{k+1}\xi_{k+1}\xi^{T}_{k+1}\mathcal{K}^{T}_{k+1}+\mathcal{K}_{k+1}\mathbf{\Psi}_{k+1}\mathcal{R}_{k+1}\mathbf{\Psi}^{T}_{k+1}\mathcal{K}^{T}_{k+1}\\ \leqslant&\varpi_{1}(I+\mathcal{K}_{k+1}\mathbf{\Psi}_{k+1}\mathbf{C}_{k+1})((\mathbf{P}^{-}_{k+1})^{-1}-\alpha_{2}\bar{\mathbf{H}}^{T}_{k+1}\bar{\mathbf{H}}_{k+1})^{-1}\\ &\times(I+\mathcal{K}_{k+1}\mathbf{\Psi}_{k+1}\mathbf{C}_{k+1})^{T}+\varpi_{1}\alpha_{2}^{-1}\mathcal{K}_{k+1}\mathbf{\Psi}_{k+1}\bar{\mathbf{G}}_{k+1}\bar{\mathbf{G}}^{T}_{k+1}\mathbf{\Psi}^{T}_{k+1}\mathcal{K}^{T}_{k+1}\\ &+\mathcal{K}_{k+1}\mathbf{\Psi}_{k+1}\mathcal{R}_{k+1}\mathbf{\Psi}^{T}_{k+1}\mathcal{K}^{T}_{k+1}+\varpi_{2}\vec{\varrho}_{k}\mathcal{K}_{k+1}\mathcal{K}^{T}_{k+1}.\end{aligned}\tag{32}$$

The proof is thus complete.

Theorem 2 *The filter gain can be given by*

$$\mathbf{K}_{ij,k+1}=\begin{cases}\mathcal{K}_{ij,k+1}a_{ij}^{-1}, & a_{ij}\neq 0\\ 0, & a_{ij}=0.\end{cases}\tag{33}$$

Proof of Theorem 2. Taking the partial for the upper bound (23) with respect to $\mathcal{K}_{k+1}$ yields

$$\frac{\partial\mathbf{\Sigma}^{+}_{k+1}}{\partial\mathcal{K}_{k+1}}=2(I+\mathcal{K}_{k+1}\mathbf{\Psi}_{k+1}\mathbf{C}_{k+1})\mathbf{V}_{k+1}+2\mathcal{K}_{k+1}\mathbf{U}_{k+1}\tag{34}$$

where

$$\mathbf{V}_{k+1}=\varpi_{1}((\mathbf{\Sigma}^{-}_{k+1})^{-1}-\alpha_{2}\bar{\mathbf{H}}^{T}_{k+1}\bar{\mathbf{H}}_{k+1})^{-1}\mathbf{C}^{T}_{k+1}\mathbf{\Psi}^{T}_{k+1}.$$

Letting $\frac{\partial\mathbf{\Sigma}^{+}_{k+1}}{\partial\mathcal{K}_{k+1}}=0$, one has

$$\mathcal{K}_{k+1}=-\mathbf{V}_{k+1}\mathbf{W}^{-1}_{k+1}\tag{35}$$

where

$$\mathbf{W}_{k+1}\triangleq\mathbf{\Psi}_{k+1}\mathbf{C}_{k+1}\mathbf{V}_{k+1}+\mathbf{U}_{k+1}.$$

Furthermore, we have

$$\mathcal{K}_{k+1}=\sum_{i=1}^{N}\mathbf{E}_{i}\mathbf{K}_{k+1}\mathcal{A}_{i}.\tag{36}$$

Therefore, it is easy to conclude that

$$[\mathbf{K}_{i1,k+1},\mathbf{K}_{i2,k+1},\cdots,\mathbf{K}_{iN,k+1}]=[\mathcal{K}_{i1,k+1},\mathcal{K}_{i2,k+1},\cdots,\mathcal{K}_{iN,k+1}]\mathcal{A}_{i}^{\dagger}\tag{37}$$

where $\mathcal{A}_{i}^{\dagger}$ is the Moore-Penrose pseudoinverse of $\mathcal{A}_{i}$. The proof is complete.

Remark 1 *In this paper, we consider the distributed filtering problem for sensor networks with the uniform quantization and the privacy protection. The network consists of a large number of spatially distributed intelligent nodes capable of sensing environment information, processing data, and communicating with neighboring nodes. To effec-*

tively address bandwidth constraints, uniform quantization is introduced in inter-node communication. Meanwhile, we introduce an output mask function to protect the privacy of measurement data. It is noteworthy that, in our main theorems, key elements of the system are comprehensively considered: the selection of quantization parameters, output mask function, the influence of network topology, and linearization errors, all of which are closely related to engineering practice.

Remark 2 *This paper proposes an innovative distributed recursive filtering framework that addresses data privacy protection and resource allocation in network communications through the introduction of output mask functions and scaled uniform quantization techniques. In Theorem 1, a tight upper bound for the filtering error covariance is analytically derived, which directly relates to the output mask function and quantization level. In Theorem 2, we develop a recursive method for solving the desired filter gain matrix by means of Riccati-like difference equations. The effectiveness and practical applicability of the proposed filter design approach are rigorously validated through a three-tank simulation, confirming both theoretical soundness and engineering viability. Future work will investigate advanced privacy protection technologies, such as differential privacy and homomorphic encryption, for more complex nonlinear systems to strengthen privacy safeguards without compromising estimation accuracy.*

4. Numerical Simulations

In this section, an experimental simulation is conducted on an internet-based three-tank system [36] to validate the effectiveness and applicability of the proposed distributed filtering strategy in a networked environment. As illustrated in [35], the system comprises three tanks, where each has an equivalent cross-sectional area G_a and is connected by two cylindrical pipes with a specific cross-sectional area G_n. Tanks 1 and 2 are both equipped with pumps that supply water at designated flow rates $W_1(t)$ and $W_2(t)$. Furthermore, two sensors are installed to measure the water levels in each tank.

In the simulation, it is assumed that the water levels in the three tanks satisfy the condition $\hbar_1(t) > \hbar_3(t) > \hbar_2(t)$, meaning that water always flows from Tank 1 to Tank 2 via Tank 3. Based on the ``mass balance principle'', the dynamic behavior of the tank levels can be described by the following differential equations:

$$\begin{aligned}\dot{\hbar}_1(t) &= \frac{1}{G_a}(W_1(t) - W_{13}(t)) + b_{11}w_1(t)\\ \dot{\hbar}_2(t) &= \frac{1}{G_a}(W_2(t) + W_{32}(t) - W_{20}(t)) + b_{12}w_2(t)\\ \dot{\hbar}_3(t) &= \frac{1}{G_a}(W_{13}(t) - W_{32}(t)) + b_{13}w_3(t).\end{aligned} \tag{38}$$

Here, $W_{ij}(t)$ represents the water flow rate from the ith tank to the jth tank, and can be calculated as

$$W_{ij}(t) = \chi_i G_n \mathrm{sign}(\hbar_i(t) - \hbar_j(t)) \sqrt{2g|\hbar_i(t) - \hbar_j(t)|} \tag{39}$$

where χ_i is the outflow coefficient of pipe i, G_n is the cross section area of the connection pipe, and $g = 9.8\mathrm{m/s}^2$ is the gravity acceleration. The term $W_{20}(t)$ represents the outflow rate from tank 2 and is given by

$$W_{20}(t) = \chi_2 G_n \sqrt{2g\hbar_2(t)}. \tag{40}$$

Additionally, $w_i(t)$ denotes the process noise with the intensity coefficient b_{1i}. Substituting the explicit forms of the parameters into (38) yields the following expression:

$$\begin{aligned}\dot{\hbar}_1(t) &= \frac{1}{G_a}\Big(-\chi_1 G_n \sqrt{2g(\hbar_1(t) - h_3(t))} + W_1(t)\Big) + b_{11}w_1(t)\\ \dot{\hbar}_2(t) &= \frac{1}{G_a}\Big(\chi_3 G_n \sqrt{2g(\hbar_3(t) - \hbar_2(t))} - \chi_2 G_n \sqrt{2g\hbar_2(t)} + W_2(t)\Big) + b_{12}w_2(t)\\ \dot{\hbar}_3(t) &= \frac{1}{G_a}\Big(\chi_1 G_n \sqrt{2g(\hbar_1(t) - \hbar_3(t))} - \chi_3 G_n \sqrt{2g(\hbar_3(t) - \hbar_2(t))}\Big) + b_{13}w_3(t).\end{aligned} \tag{41}$$

By applying the Euler discretization method [36] to the continuous-time state equation at each sampling instant t_k, the corresponding approximate discrete-time counterpart is given by

$$\begin{aligned}
\hbar_1(t_{k+1}) &= \hbar_1(t_k) - \frac{TG_n}{G_a}\chi_1\sqrt{2g(\hbar_1(t_k)-\hbar_3(t_k))} \\
&\quad + \frac{T}{G_a} + \frac{T}{G_a}W_1(t_k) + Tb_{11}w_1(t_k) \\
\hbar_2(t_{k+1}) &= \hbar_2(t_k) + \frac{TG_n}{G_a}\chi_3\sqrt{2g(\hbar_3(t_k)-\hbar_2(t_k))} \\
&\quad - \frac{TG_n}{G_a}\chi_2\sqrt{2g\hbar_2(t_k)} + \frac{T}{G_a}W_2(t_k) + Tb_{12}w_2(t_k) \\
\hbar_3(t_{k+1}) &= \hbar_2(t_k) + \frac{TG_n}{G_a}\chi_1\sqrt{2g(\hbar_1(t_k)-\hbar_3(t_k))} \\
&\quad - \frac{TG_n}{G_a}\chi_3\sqrt{2g(\hbar_3(t_k)-\hbar_2(t_k))} + Tb_{13}w_3(t_k).
\end{aligned} \tag{42}$$

In this context, T represents the constant sampling interval, defined as $T \triangleq t_{k+1} - t_k$. Similarly, the measurement equation is formulated in the following manner:

$$\begin{aligned}
y_1(t_k) &= (1+\sin(t_k))\hbar_1(t_k) + b_{21}v_1(t_k) \\
y_2(t_k) &= \hbar_2(t_k) + b_{22}v_2(t_k)
\end{aligned} \tag{43}$$

where $\sin(t_k)$ stands for the measurement error and $v_i(t_k)$ is the measurement noise with the intensive coefficient b_{2i}.

For simplicity, in the following sections, we will use k as an abbreviation for t_k. Additionally, we assume that the process noises w_{ik} $(i = 1,2,3)$ are identical and follow truncated Gaussian distributions. Specifically, w_{ik} $(i = 1,2,3)$ are drawn from a Gaussian distribution with zero mean and variance Q_k. Similarly, we make the same assumption about the measurement noises v_{ik} $(i = 1,2)$, that is, $v_{ik} = v_k \sim \mathcal{N}(0,R_k)$ $(i = 1,2)$. Based on (41) to (43), the system parameters are outlined as follows:

$$\begin{aligned}
B_{1k} &= \begin{bmatrix} b_{11} & b_{12} & b_{13}\end{bmatrix}^T = \begin{bmatrix}1 & 1 & 0.05\end{bmatrix}^T, B_{2k} = \begin{bmatrix} b_{21} & b_{22}\end{bmatrix}^T = \begin{bmatrix}1 & 1\end{bmatrix}^T \\
C_k &= \begin{bmatrix} 1+0.1\sin(k) & 0 & 0 \\ 0 & 1 & 0\end{bmatrix}, Q_k = 0.0001, R_k = 0.05
\end{aligned} \tag{44}$$

Other system parameters are set as $G_a = 254\text{cm}^2$, $G_n = 8s$, $Q_1 = 20\text{cm}^2$, $Q_2 = 21\text{cm}^3$, $\chi_1 = 0.48$, $\chi_2 = 0.58$, and $\chi_3 = 0.48$.

The system state is measured by four sensors with the following topology structure:

$$\mathcal{A} = \begin{bmatrix} 1 & 0 & 0.5 & 0.5 \\ 0.5 & 1 & 0 & 0.5 \\ 0 & 0.5 & 1 & 0.5 \\ 0.1 & 0.5 & 0 & 1 \end{bmatrix}. \tag{45}$$

For the output mask function (4), we set $\psi_i = 0.2$, $\nu_i = 0.2$, $\theta_i = \begin{bmatrix}0.5 \\ 0.5\end{bmatrix}$ and $\varepsilon_i = 0.12$. For the uniform quantizaiton (5), let the quantization range $M = 1$, the quantization level $\rho = 100$ and the adjustable parameter $\varrho_i = 2$. The following initial values are given $x_0 = \begin{bmatrix}0.45 & 0.14 & 0.18\end{bmatrix}^T$, $\hat{x}^+_{i,0} = \begin{bmatrix}0.05 & 0.04 & 0.08\end{bmatrix}^T$ and $\mathbf{\Sigma}^+_{i,0} = I$. For the Taylor expansion, set $\mathbf{G}_i = 0.5I$, $\mathbf{H}_i = 0.1I$, $\bar{\mathbf{G}}_i = 0.1I$, $\bar{\mathbf{H}}_i = 0.1I$, $\alpha_1 = \alpha_2 = 0.1$ and $\kappa = 15$. The simulation results are shown in Figures 1–3 where the estimation trajectories track the real state. It can be observed that the proposed distributed recursive filtering algorithm demonstrates high accuracy and robustness in estimating all three states. The algorithm effectively handles the challenges posed by quantization effects and privacy protection mechanisms.

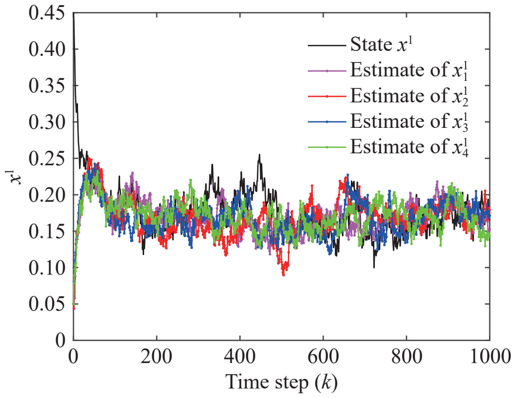

Figure 1. The estimation of x_k^1.

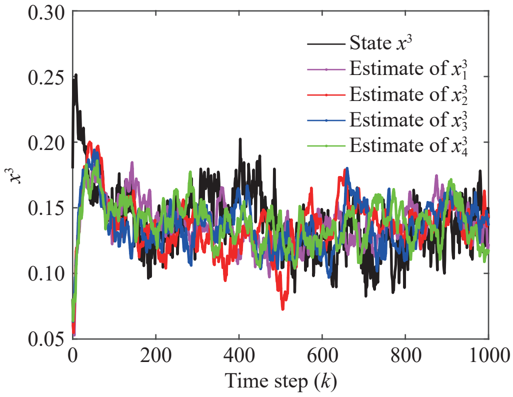

Figure 3. The estimation of x_k^3.

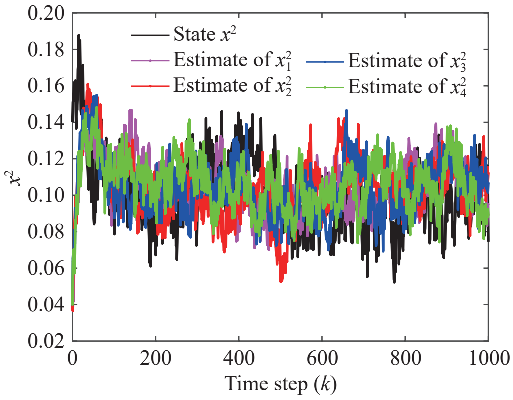

Figure 2. The estimation of x_k^2.

5. Conclusions

This paper has addressed the distributed recursive filtering issue for state-saturated systems in networked environments. An output mask function has been used to safeguard privacy during sensor node interactions and scaled uniform quantization has been employed to enhance communication efficiency and optimize network resource usage. The study focuses on designing a distributed recursive filter to ensure that the filtering error covariance is bounded over a finite horizon. By using Riccati-like equations, an upper bound for the filtering error has been derived, which is influenced by the network topology, the mask function, and the quantization level. The gain matrix has been determined recursively, and the effectiveness of the proposed filtering algorithm has been validated through a three-tank simulation example.

Author Contributions: Youyin Hu: Conceptualization, Methodology, Software, Writing-original draft; **Chen Zhang**: Methodology, Software, Writing-review & editing; **Shuai Liu**: Conceptualization, Methodology, Writing-

original draft, Supervision, Writing-review & editing.

Funding: This work was supported in part by the National Natural Science Foundation of China under Grant 62473261, and the Natural Science Foundation of Shanghai of China under Grant 24ZR1453800.

Data Availability Statement: Not applicable.

Conflicts of Interest: The authors declare no conflict of interest.

References

1. Li, X.H.; Ye, D. Dynamic event-triggered distributed filtering design for interval type-2 fuzzy systems over sensor networks under deception attacks. Int. J. Syst. Sci. **2023**, *54*, 2875–2890. doi:10.1080/00207721.2020.1871528
2. Wang, Y.A.; Shen, B.; Zou, L.; *et al*. A survey on recent advances in distributed filtering over sensor networks subject to communication constraints. Int. J. Netw. Dyn. Intell. **2023**, *2*, 100007. doi:10.53941/ijndi0201007
3. Hou, N.; Wang, Z.D.; Dong, H.L.; *et al*. Distributed fault estimation over sensor networks with randomly switching topologies under binary encoding scheme. IEEE Trans. Netw. Sci. Eng. **2024**, *11*, 2715–2728. doi:10.1109/TNSE.2023.3348432
4. Geng, H.; Wang, Z.D.; Ma, L.F.; *et al*. Distributed filter design over sensor networks under try-once-discard protocol: Dealing with sensor-bias-corrupted measurement censoring. IEEE Trans. Syst., Man, Cybern.: Syst. **2024**, *54*, 3032–3043. doi:10.1109/TSMC.2024.3354883
5. Liu, Q.Y.; Wang, Z.D.; Dong, H.L.; *et al*. Distributed Kalman filtering under two-bitrate periodic coding strategies. IEEE Trans. Automat. Control. **2024**, *69*, 8633–8646. doi:10.1109/TAC.2024.3413009
6. Chen, W.; Wang, Z.D.; Zou, L.; *et al*. A regularized least-squares approach to event-based distributed robust filtering over sensor networks. Automatica. **2024**, *163*, 111604. doi:10.1016/j.automatica.2024.111604
7. Han, F.; Wang, Z.D.; Liu, H.J.; *et al*. A recursive matrix inequality approach to distributed filtering over binary sensor networks: Handling amplify-and-forward relays. IEEE Trans. Netw. Sci. Eng. **2024**, *11*, 1347–1362. doi:10.1109/TNSE.2023.3322378
8. Kalman, R.E. A new approach to linear filtering and prediction problems. *J. Basic Eng*. 1960, *82*, 35–45. doi:10.1115/1.3662552
9. Feng, S.; Li, X.G.; Zhang, S.; *et al*. A review: State estimation based on hybrid models of Kalman filter and neural network. Syst. Sci. Control Eng. **2023**, *11*, 2173682. doi:10.1080/21642583.2023.2173682
10. Liu, D.; Wang, Z.D.; Liu, Y.R.; *et al*. Extended Kalman filtering subject to random transmission delays: Dealing with packet disorders. Inf. Fusion. **2020**, *60*, 80–86. doi:10.1016/j.inffus.2020.02.006
11. Liu, S.; Wang, Z.D.; Hu, J.; *et al*. Protocol-based extended Kalman filtering with quantization effects: The Round-Robin case. Int. J. Robust Nonlinear Control. **2020**, *30*, 7927–7946. doi:10.1002/rnc.5205
12. Wang, Z.D.; Liu, X.H.; Liu, Y.R.; *et al*. An extended Kalman filtering approach to modeling nonlinear dynamic gene regulatory networks via short gene expression time series. IEEE/ACM Trans. Comput. Biol. Bioinf. **2009**, *6*, 410–419. doi:10.1109/TCBB.2009.5
13. Moradi, A.; Venkategowda, N.K.D.; Talebi, S.P.; *et al*. Privacy-preserving distributed Kalman filtering. IEEE Trans. Signal Process. **2022**, *70*, 3074–3089. doi:10.1109/TSP.2022.3182590
14. Rajagopal, A.; Chitraganti, S. State estimation and control for networked control systems in the presence of correlated packet drops. Int. J. Syst. Sci. **2023**, *54*, 2352–2365. doi:10.1080/00207721.2023.2230225
15. Wang, L.C.; Wang, Z.D.; Liu, S.; *et al*. Unscented Kalman filtering over full-duplex relay networks under binary encoding schemes. IEEE Trans. Automat. Control. **2025**, *70*, 3441–3448. doi:10.1109/TAC.2024.3521281
16. Zheng, S.S.; Liu, S.; Wang, L.C. Event-triggered distributed optimization for model-free multi-agent systems. Front. Inform. Technol. Electron. Eng. **2024**, *25*, 214–224. doi:10.1631/FITEE.2300568
17. Wang, L.C.; Wang, Z.D.; Zhao, D.; *et al*. Recursive filtering for discrete-time stochastic complex networks under bit-rate constraints: A locally minimum variance approach. IEEE Trans. Automat. Control. **2024**, *69*, 3441–3448. doi:10.1109/TAC.2023.3349102
18. Wang, L.C.; Wang, Z.D.; Zhao, D.; *et al*. Stabilization of linear discrete-time systems over resource-constrained networks under dynamical multiple description coding scheme. Automatica. **2023**, *156*, 111160. doi:10.1016/J.AUTOMATICA.2023.111160
19. Zhang, R.; Liu, H.J.; Liu, Y.F.; *et al*. Dynamic event-triggered state estimation for discrete-time delayed switched neural networks with constrained bit rate. Syst. Sci. Control Eng. **2024**, *12*, 2334304. doi:10.1080/21642583.2024.2334304
20. Xing, S.Y.; Luan, H.; Deng, F.Q. Exponential synchronisation for delayed Clifford-valued coupled switched neural networks via static event-triggering rule. Int. J. Syst. Sci. **2024**, *55*, 1114–1126. doi:10.1080/00207721.2023.2301498
21. Li, X.; Song, Q.K.; Liu, Y.R. Optimal control and non-zero-sum differential game for Hurwicz model considering uncertain dynamic systems with multiple input delays. Int. J. Syst. Sci. **2023**, *54*, 1676–1693. doi:10.1080/00207721.2023.2208133
22. Liu, N.; Qian, W. Stability analysis of low-voltage direct current system with time-varying delay. Syst. Sci. Control Eng. **2024**, *12*, 2293918. doi:10.1080/21642583.2023.2293918
23. Liu, Y.; Wang, Z.D.; Lin, H.; *et al*. Encoding-decoding-based fusion estimation with filter-and-forward relays and stochastic measurement delays. Inf. Fusion. **2023**, *100*, 101963. doi:10.1016/j.inffus.2023.101963
24. Li, J.; Suo, Y.H.; Chai, S.C.; *et al*. Resilient and event-triggered control of singular Markov jump systems against cyber attacks. Int. J. Syst. Sci. **2024**, *55*, 222–236. doi:10.1080/00207721.2023.2269293
25. Sakthivel, R.; Parivallal, A.; Kwon, O.M.; *et al*. Observer-based leader-following cluster consensus for positive multi-agent systems with input time-varying delay. Int. J. Syst. Sci. **2024**, *55*, 3017–3031. doi:10.1080/00207721.2024.2364294
26. Wu, Y.B.; Niu, Y.G.; Yang, Y.K. Security sliding mode control for T-S fuzzy systems under attack probability-dependent dynamic round-robin protocol. Int. J. Syst. Sci. **2024**, *55*, 926–940. doi:10.1080/00207721.2023.2301037
27. Hu, J.; Sun, Q.Y.; Wang, R.; *et al*. An improved privacy-preserving consensus strategy for AC microgrids based on output mask approach and node decomposition mechanism. IEEE Trans. Automat. Sci. Eng. **2024**, *21*, 642–651. doi:10.1109/TASE.2022.3217677
28. Chen, W.; Wang, Z.D.; Hu, J.; *et al*. Privacy-preserving distributed economic dispatch of microgrids using edge-based additive per-

turbations: An accelerated consensus algorithm. IEEE Trans. Syst., Man, Cybern.: Syst. **2024**, *54*, 2638–2650. doi:10.1109/TSMC.2023.3344885
29. Chen, W.; Wang, Z.D.; Liu Q.Y.; *et al*. A new privacy-preserving average consensus algorithm with two-phase structure: Applications to load sharing of microgrids. Automatica. **2024**, *167*, 111715. doi:10.1016/j.automatica.2024.111715
30. Gao, C.; Wang, Z.D.; He, X.; *et al*. Sampled-data-based fault-tolerant consensus control for multi-agent systems: A data privacy preserving scheme. Automatica. **2021**, *133*, 109847. doi:10.1016/j.automatica.2021.109847
31. Chen, W.; Wang, Z.D.; Dong, H.L.; *et al*. Privacy-preserving distributed economic dispatch of microgrids over directed networks via state decomposition: A fast consensus algorithm. IEEE Trans. Ind. Inf. **2024**, *20*, 4092–4102. doi:10.1109/TII.2023.3321027
32. Wang, W.; Ma, L.F.; Rui, Q.Q.; *et al*. A survey on privacy-preserving control and filtering of networked control systems. Int. J. Syst. Sci. **2024**, *55*, 2269–2288. doi:10.1080/00207721.2024.2343734
33. Altafini, C. A system-theoretic framework for privacy preservation in continuous-time multiagent dynamics. Automatica. **2020**, *122*, 109253. doi:10.1016/j.automatica.2020.109253
34. Wang, A.J.; He, H.B.; Liao, X.F. Event-triggered privacy-preserving average consensus for multiagent networks with time delay: An output mask approach. IEEE Trans. Syst., Man, Cybern.: Syst. **2021**, *51*, 4520–4531. doi:10.1109/TSMC.2019.2939680
35. Wang, L.C.; Wang, Z.D.; Shen, B.; *et al*. Recursive filtering with measurement fading: A multiple description coding scheme. IEEE Trans. Automat. Control. **2021**, *66*, 5144–5159. doi:10.1109/TAC.2020.3034196
36. He, X.; Wang, Z.D.; Wang, X.F.; *et al*. Networked strong tracking filtering with multiple packet dropouts: Algorithms and applications. IEEE Trans. Ind. Electron. **2014**, *61*, 1454–1463. doi:10.1109/TIE.2013.2261038

Citation: Y.Y. Hu; C. Zhang; S. Liu. Privacy-Preserving Distributed Recursive Filtering for State-Saturated Systems with Quantization Effects. *International Journal of Network Dynamics and Intelligence*. 2025, 4(2), 100012. doi: 10.53941/ijndi.2025.100012